2023 IEEE International Conference on Robotics and Automation (ICRA 2023)
May 29 - June 2, 2023. London, UK

3D-Printed Adaptive Microgripper Driven by Thin-Film NiTi Actuators

Sukjun Kim, Sarah Bergbreiter

Abstract— **Creating microscale actuated mechanisms in 3D space is extremely challenging due to limitations in microfabrication processes. In this work, we present a 3D-printed adaptive microgripper that is driven by thin-film NiTi microactuators with 3D-printed linkage mechanisms. The microgripper's fingers are passively adaptive so that the microgripper can provide conformal gripping on 3D objects. The microgripper can move its fingers by 225 µm and apply a blocking force of 30 µN per one finger when 20 mA was applied to the NiTi actuators. The microgripper was also integrated onto a printed circuit board with a current regulating circuit and a 9 V battery. Since the NiTi actuator requires a low voltage for actuation, the microgripper could be integrated with simple and affordable electronics. The fully integrated microgripper system was demonstrated playing with a shape sorting box at the microscale for the first time.**

I. INTRODUCTION

Microrobotic systems that can interact with physical environments require efficient and high work density microactuators as well as effective mechanisms for translating input actuation into desired output motion in three-dimensional (3D) space. Ultimately, these mechanisms also need to be integrated with electronic components (e.g., microcontrollers and power supplies) to achieve higher robot autonomy [1]. However, creating actuated mechanisms at the small scale and developing the mechanisms into integrated robotic systems is challenging due to limited approaches for manufacturing and integration at the microscale.

Although various microscale actuated mechanisms have been demonstrated [2]–[6], the manufacturing of these mechanisms involved microfabrication or laser patterning which limits the design space of the mechanism to two-dimensional (2D) space. Therefore, a post processing with manual assembly was inevitable to develop more complex mechanisms and robotic systems in 3D space. However, it is challenging to manually assemble tiny components, which also could affect the yield of the manufacturing process.

Recently introduced 3D printing technology at the microscale using two photon polymerization (TPP) can circumvent some of these challenges. Since TPP can directly fabricate complex 3D features with sub-micron resolution, 3D structures can be designed for microscale mechanisms and microrobots in a way that does not require any post-processing. These capabilities of TPP have enabled microswimmers [7], legged microrobots [8], [9], and 3D microactuators and mechanisms [10]–[14], which are extremely challenging to achieve using traditional microfabrication processes or even using folding-based processes at these size scale [15]. The 3D microactuators in [10]–[12] (e.g., thermal, SMA, and electrostatic actuators) are even compatible with small and lightweight power electronics [16], which enables further integration for autonomous microrobots.

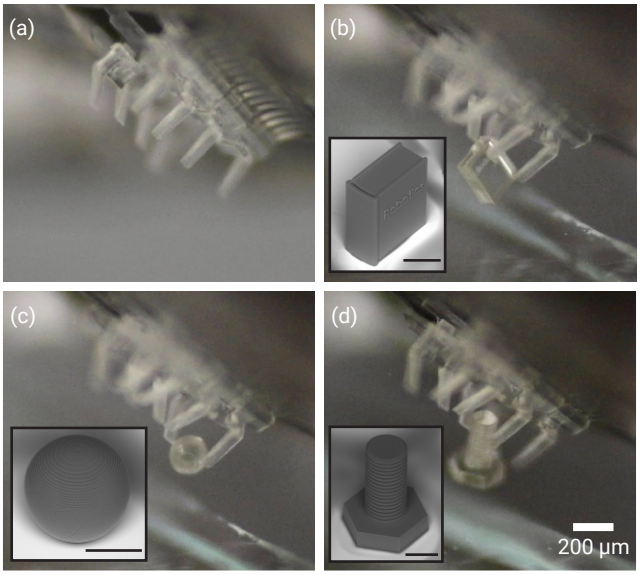

Fig. 1. A NiTi actuator driven 3D-printed microgripper. Microscale objects with various shapes can be gripped. (a) Gripper at idle. (b) Gripping a book, (c) a ball, and (d) a bolt. Insets show SEM images of each object. The scale bar in insets represent 100 µm.

In this work, we present a 3D-printed adaptive microgripper that is driven by thin-film NiTi microactuators as shown in Fig. 1. NiTi can provide high work density actuation by taking advantage of the shape memory effect [17] and can operate at high bandwidths when fabricated as a thin-film [18], which makes thin-film NiTi an attractive option for small-scale robotic systems. A primary contribution of this work is the integration of 3D-printed linkage mechanisms with the thin-film NiTi. By taking advantage of the basic bi-layer NiTi actuators that were previously studied in [12], [13], a gripper mechanism with compliant flexure joints was actuated to grip various microscale objects (Fig. 1(b), (c), and (d)). Two versions of this microgripper were tested. In the first design of a rigid microgripper, 4 fingers of the microgripper on each side were rigidly connected that the microgripper behaves similar to a simple one degree of freedom (DoF) gripper. A secondary contribution of this paper is the design of a second adaptive microgripper. Each finger of the adaptive gripper could individually move and passively adapt

This work was supported by Air Force Office of Scientific award number FA9550-19-1-0386.

The authors are with the Department of Mechanical Engineering, Carnegie Mellon University, Pittsburgh, PA 15213 USA (e-mail: sukjunk@andrew.cmu.edu; sbergbre@andrew.cmu.edu).

to a surface of an object resulting in conformal gripping. To better understand a behavior of the two microgrippers, gripper motion and force were characterized. In addition, temperature at the gripper tip was characterized to ensure heating of the NiTi would not significantly affect the gripped part. A third contribution is a fully integrated microgripper system powered by an off-the-shelf battery. By integrating the microgripper onto a printed circuit board (PCB) with a current regulating circuit, the microgripper was demonstrated playing with a microscale shape sorting box for the first time.

II. METHODS

A. NiTi actuator design

The microgrippers in this work were actuated by thin-film NiTi shape memory alloy actuators that were previously studied in [12], [13], [19]. This bi-layer NiTi actuator has 0.93 µm thick sputtered NiTi film at the bottom and a 15 µm thick 3D-printed polymer layer on top (Fig 2(a)). The actuator is initially bent up due to the shrinkage of the polymer and thermal stress during fabrication. When the actuator is heated up, both the shape memory effect and the coefficient of thermal expansion mismatch between the two layers contribute to actuation. Since the NiTi film memorizes a flat shape during sputtering, the NiTi layer flattens when the temperature of the actuator exceeds a phase transition temperature of NiTi ($A_s \approx 60\,°C$ [12]). In addition, the coefficient of thermal expansion of the polymer is about an order of magnitude higher than that of NiTi [19] so the polymer layer also expands more than the NiTi layer when heated. Therefore, when the actuator is heated, both effects induce the actuator to bend downward. For these microgrippers, eight NiTi bi-layer actuators are designed in parallel. As shown in the inset of Fig. 2(a), the NiTi layer has 8 U-shape paths in parallel, and the paths are electrically connected in series. Each U-shape path defines one actuator. When current flows through the NiTi paths, the temperature of the actuators increases by resistive heating (Joule heating). Since the actuators are electrically connected in series, a single input is required to power all 8 actuators. The length of each actuator and the width of the U-shape paths are 250 µm and 45 µm respectively.

B. Gripper mechanism design

A linkage mechanism with compliant flexure joints was designed for each finger of the microgripper. The finger mechanism of the microgripper is inspired by the Scott-Russell linkage mechanism which changes the direction of a linear motion. When the NiTi actuator moves up and down in the z-axis, the linkage mechanism translates the actuator movement into the microgripper movement in y-axis (Fig. 2(a)). Fig. 2(b) shows a SEM image of the fabricated micro-gripper mechanism with the NiTi actuators. Each component of the mechanism is false-colored so the components can be easily compared with Fig. 2(a). Two adjacent NiTi actuators with 4 fingers each are used in each microgripper. Therefore, each microgripper has 8 fingers in total as shown in Fig. 2(b). The fingers are designed to be interdigitated due to the residual stress from the manufacturing process.

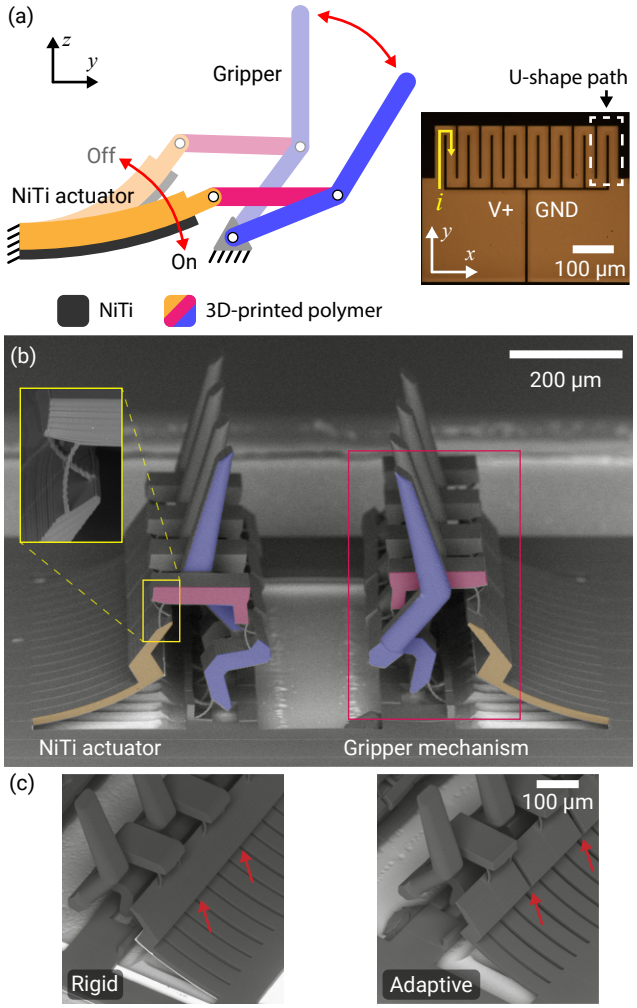

Fig. 2. A microscale gripper mechanism driven by NiTi actuators. (a) A schematic of the actuator and the mechanism from the side view. Bi-layer NiTi actuator drives the gripper mechanism. Inset shows the top view of the NiTi layer patterned on a silicon wafer. 8 U-shape paths are designed in parallel while they are electrically connected in series. (b) A SEM image of the fabricated microgripper. Cross-spring pivot joints are designed for the rotational joints between the links. (c) Two designs of the gripper are studied. Left: A rigid gripper. All 4 fingers are rigidly connected at the tip of the NiTi actuators. Right: An adaptive gripper. 4 fingers are separated as indicated with red arrows which can adapt to the shape of an object.

The cross-spring pivot joint [20] is utilized for rotational joints between the linkages. Compliant flexure joints were chosen over pin joints since pin joints need to overcome friction which can be relatively large when compared to applied forces at small scales. The inset of Fig. 2(b) shows the fabricated cross-spring pivot joints. The length and the thickness of each flexure are 50 µm and 2 µm, respectively. The joint width of one flexure is 25 µm and the intersection angle between the cross springs was 53°.

Two microgripper designs are studied in this work as shown in Fig. 2(c): rigid and adaptive grippers. The rigid gripper has all 4 fingers on each side rigidly connected at the actuator tips, and therefore, the fingers move together as

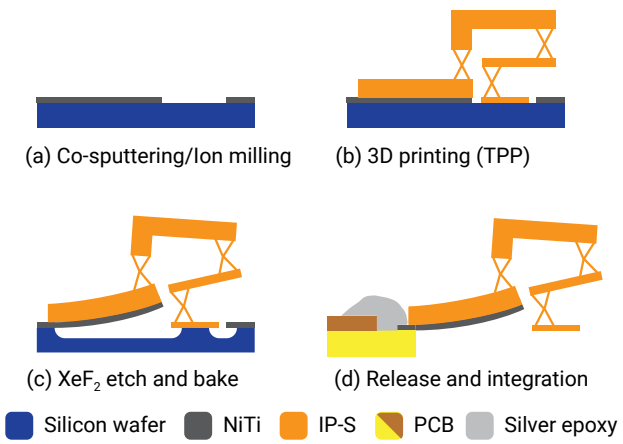

Fig. 3. Fabrication process. (a) NiTi film is co-sputtered on a silicon wafer and then is patterned by ion-milling. (b) Actuators and microgripper mechanisms are 3D-printed using two-photon polymerization (TPP). (d) The microgripper is partially released by XeF_2 etch and baked to apply thermal stress to the actuators. (e) The microgripper is fully released from the silicon wafer and glued onto a printed circuit board for integrated system.

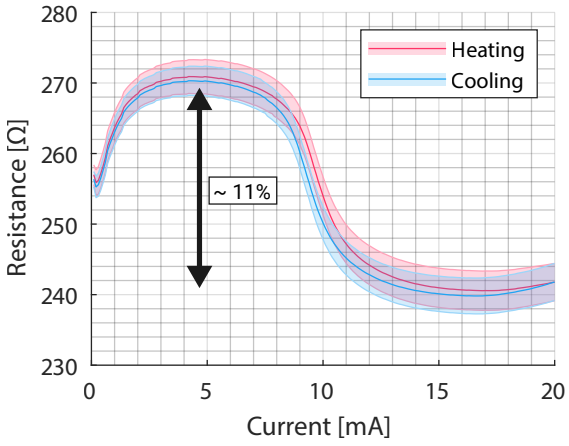

Fig. 4. NiTi resistance characterization results. The resistance of the NiTi microactuators in microgrippers was measured while sweeping the applied current. The red line shows the change in resistance while increasing the current and heating up the actuator, and the blue line shows the change in resistance while decreasing the current and cooling the actuator. The change in resistance due to the phase change of NiTi was $\sim$ 11%.

a single mechanism. This approach replicates many similar microgripper designs from past work that use rigid end effectors [21]–[23]. The fingers are separated from each other in the adaptive gripper design as the red arrows indicate in Fig. 2(c). Thus, 4 independent fingers are driven by a single input. When the gripper is actuated, each finger can individually move and apply force to an object by adapting to a shape of an object, which allows for more conformal gripping.

C. Fabrication

A fabrication process for the NiTi actuator driven microgripper is based on the method previously developed in [12]. A combination of microfabrication with 3D printing allows rapid prototyping of complex 3D designs which is extremely challenging to achieve with traditional microfabrication. First, a NiTi thin-film was co-sputtered on a silicon wafer at 700 °C and then patterned with ion-milling (Fig. 3(a)). The processed wafer was diced, and actuators with microgripper mechanisms were directly 3D-printed over the NiTi layer using TPP (Nanoscribe Photonic Professional GT +, Nanoscribe Gmbh). A negative-tone photoresist (IP-S, Nanoscribe) was used with a 25X/NA 0.8 objective lens (Zeiss) in Dip-In Laser Lithography (DiLL) mode. A laser power and a scanning speed of 35 mW and 100 000 µm s^{-1} respectively were used during printing. However, it should be noted that the laser power was reduced to 22.5 mW while printing near the NiTi layer to avoid generating bubbles on a high reflective surface. 3D-printed structures were developed in propylene glycol methyl ether acetate (PGMEA, Sigma-Aldrich) for 20 min, then immersed in isopropyl alcohol (IPA, VWR) for 2 min to remove any excess photoresist and developer. The 3D-printed structures were dried in air at room temperature after development (Fig. 3(b)).

To release the NiTi actuators and the mechanisms from the substrate, the silicon was etched with XeF_2 (SPTS Xactix, Xetch). Once the actuators and mechanisms were released, the sample was baked on a hot plate to apply thermal stress to the actuator. Due to the thermal stress and shrinkage of the 3D-printed polymer, the actuators bend up when cooled down (Fig. 3(c)). The rigid gripper and the adaptive gripper were baked at 150 °C and 180 °C respectively. Two different temperatures were used to achieve similar gripper openings for each gripper design. Finally, the microgrippers were fully released from the wafer with XeF_2 and glued onto a PCB with cyanoacrylate (Super glue, Loctite). Note that the base of the actuator and the base of the gripper mechanism are rigidly connected with 3D printed parts as shown in Fig. 2(b). The PCB was fabricated with a UV laser cutter (U3, LPKF). Electrical connection between the actuators and copper traces on the PCB was achieved with silver epoxy (8331D, MG chemicals). Finally, the PCB was integrated with a circuit through thin enamel-coated copper wires (Fig. 3(d)).

III. RESULTS

A. NiTi resistance characterization

When NiTi actuators are actuated, the actuators need to be heated above the phase transition temperature to take advantage of the shape memory effect. However, it is often challenging to directly measure the temperature of the thin-film NiTi. Instead, the change in the resistance of NiTi can be used instead as an indicator for the phase change [12], [24], [25]. As shown in Fig. 4, a current was applied to the NiTi actuators and the resistance was measured using a source-measure unit (SMU) instrument (2410, Keithley). The red and blue lines in Fig. 4 show the change in resistance while increasing and decreasing the applied current respectively. A rapid change in resistance was observed at 10 mA with a negative temperature coefficient of resistance indicating the

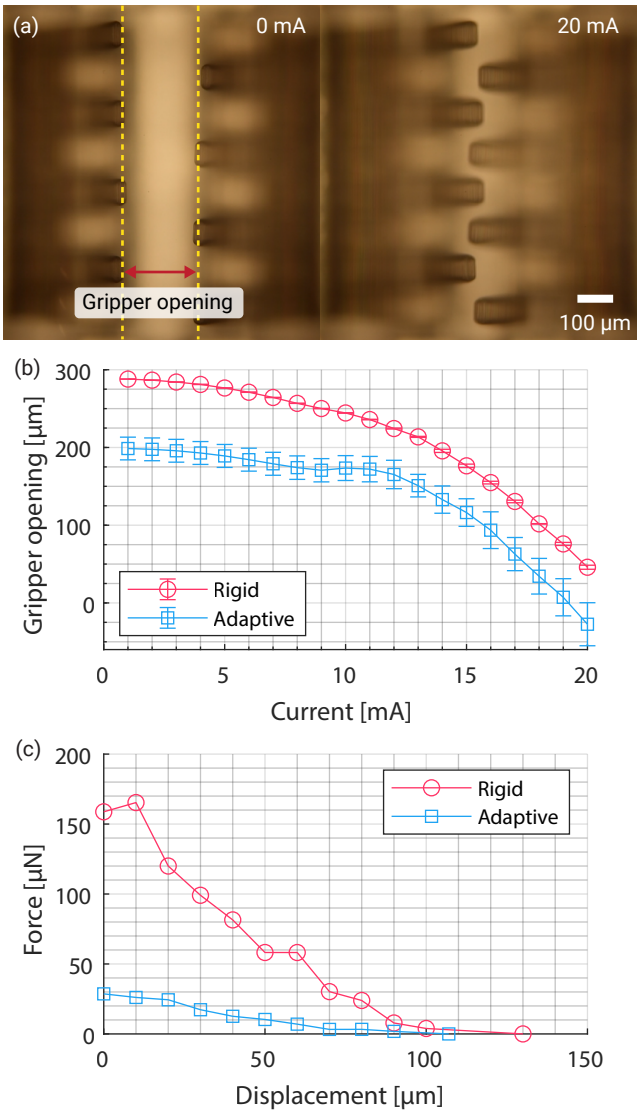

Fig. 5. Microgripper displacement and force characterization results. (a) Photographs of the microgripper from the top view showing the gripper opening. Left and right shows the gripper position at 0 and 20 mA. (b) The gripper opening with respect to applied current. (c) Force-displacement profile of a gripper's finger. The force at 0 µm is the blocking force.

phase transition of the NiTi film. Therefore, we can assume that the actuator has changed the phase from martensite to austenite when the applied current was higher than 15 mA.

B. Microgripper Displacement and Force Characterization

Understanding the force and displacement characteristics of the gripper is important to achieve an effective grip. For convenience, the microgrippers were left on the silicon wafer during the characterization (e.g. fabricated up to step (c) in Fig. 3). Fig. 5(a) shows the top view of the adaptive gripper when idle and open (left) and actuated with 20 mA and closed (right). When a current is applied to the U-shape paths on the NiTi layer, the actuators heat up and close the gripper. Currents were applied with the SMU, and the actuation was recorded with a DSLR camera (D850, Nikon) which was mounted over a probe station (S-250-6, Signatone). Both the SMU and camera were synced and controlled by Matlab. The videos were then analyzed with motion analysis software (TEMA T2020, Image Systems).

After fabrication, the gripper openings were 280 µm and 200 µm for the rigid and adaptive grippers respectively. The discrepancy between the two designs comes from the difference in the amount of silicon undercut etching and how a thermal stress was applied to each design during fabrication. As we applied higher current to the microgripper, the actuator heated up more, and therefore, the gripper openings decreased (Fig. 5(b)). When the applied current was increased above 12 mA, the gripper opening changed more rapidly which verified the shape memory effect from the NiTi layer. The gripper opening changed by 225 µm when 20 mA was applied for both designs. From the transient displacement response at 20 mA, the rise and fall time of the gripper were measured at 183 ms and 47 ms respectively. The maximum operational frequency of 4.3 Hz was calculated.

The microgripper needs to apply enough force to successfully grip, lift, and carry an object. As shown in Fig. 5(c), The force-displacement profile of each microgripper was characterized while applying 20 mA by varying the displacement. The force was measured at the tip of the finger with a force sensor (FT-NMT03, Femtotools). The force measured at 0 µm displacement represents the blocking force, and as the displacement increased, the distance between the force sensor and the tip of the finger was increased.

The blocking force of the rigid gripper was 160 µN while that of the adaptive gripper was 30 µN. This large discrepancy in force was expected due to the different designs of each microgripper. Force was measured at the tip of one finger, so the force from the rigid gripper was generated by all 8 NiTi actuators. In the case of the adaptive gripper, all 8 NiTi actuators were still engaged but some of fingers could move with a larger displacement. However, even the blocking force of a single finger from the adaptive gripper was 30 µN which can hold a 1.5 mg of mass assuming a friction coefficient of 0.5 under gravity. Considering the mass of the gripper is estimated to be 75 µg, the gripper can provide a significant gripping force at the microscale.

One of the contributions in this work is the use of the adaptive microgripper design to achieve a conformal grip of microscale objects by adapting to the shape of an object. A 3D object was gripped with both rigid and adaptive gripper to qualitatively compare two designs (Fig. 6). A leg from a dead ant was used as a test object, representing a complex small 3D object. Since the movement of one finger in the rigid gripper is constrained by that of the other fingers, one side of the rigid gripper stops when one of four fingers make contact with the object resulting in only two contact points with the object (Fig. 6(a)). On the other hand, all of the fingers in the adaptive gripper made contact with the object (Fig. 6(b)). The mechanism of each finger could individually adapt to the shape of the object and provide conformal gripping. This design follows similar principles found in grippers at larger scales [26], [27]. The adaptive gripper was used for the remaining characterization in this work.

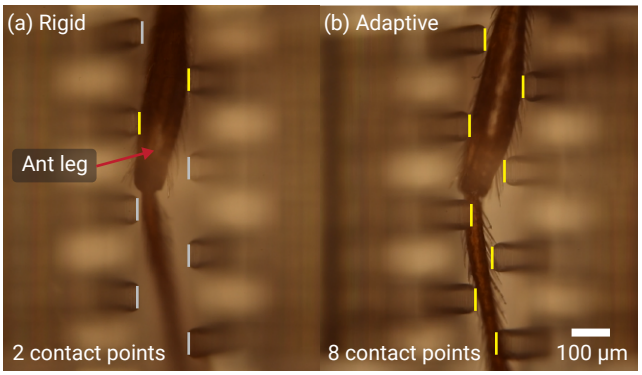

Fig. 6. Comparison between the rigid and adaptive grippers while grabbing a leg of an ant. Grippers were actuated at 20 mA. Yellow lines show the contacts between the gripper and the object. (a) Rigid gripper. Since the gripper fingers on one side move together, only 2 contact points were made. (b) Adaptive gripper. All 8 fingers made contact to an object since each finger can adapt to the shape of the object.

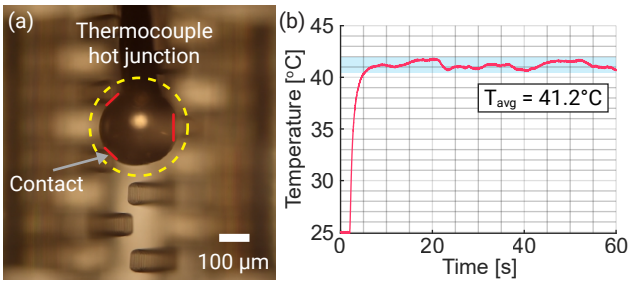

Fig. 7. Electrothermal characterization of the finger tip at 20 mA. (a) A thermocouple was used to measure the temperature of the finger tip. Yellow dotted circle and red lines indicate the hot junction of the thermocouple and the contact points between the thermocouple and the gripper fingers respectively. (b) Temperature readings from the thermocouple while actuated for 1 min. The average temperature of the thermocouple was 41.2 °C.

C. Microgripper Thermal Characterization

Since the NiTi actuators are electrothermally actuated, the temperature of the microgripper is an important consideration. High temperature at the finger tips might need to be avoided depending on applications and types of objects to grip. For example, biological samples or objects with low melting point materials could be affected during gripping. A small thermocouple (TL0201, PerfectPrime) was used to measure the temperature of the finger tip during a grip. The thermocouple was connected to a digital multimeter (34465A, Keysight), and the temperature readings were recorded. The hot junction of the thermocouple was inserted into the center of the gripper. Then, the microgripper was actuated at 20 mA for 1 min to measure the temperature at a steady state. Three fingers in the center of the microgripper made contact with the thermocouple when actuated (Fig. 7(a)). Fig. 7(b) shows the temperature readings from the thermocouple with respect to time. After 5 sec, the temperature reached the steady state, and the average of the temperature readings at the steady state was 41.2 °C. Therefore, an average temperature of a gripped object can be estimated to be around 41.2 °C. However, it has to be noted that the temperature of the finger tip could be locally higher than the average temperature since only a part of the surface of the thermocouple made contact with the finger tip.

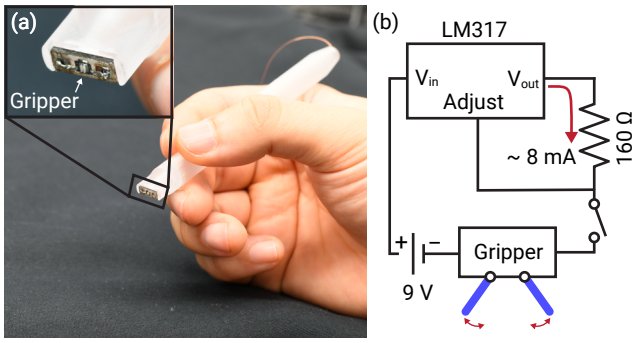

Fig. 8. Integrated microgripper system. (a) The gripper is fully released from the silicon wafer and glued onto a printed circuit board (PCB). The PCB is then glued to a 3D-printed handle, and the gripper is connected to a circuit through copper wires and silver epoxy. (b) A schematic of the circuit. A current regulator was designed to apply a constant current (∼ 8 mA) to the microgripper. Off-the-shelf 9 V battery was used to power the gripper.

D. Integrated system

Integrating microrobotic systems with electronics to achieve higher robot autonomy is challenging since some microrobots need to stay on silicon wafers or require a high voltage for actuation. However, the 3D printed microgripper with thin-film NiTi actuators can be easily released from the substrate and transferred to desired frameworks (e.g., PCB). NiTi microactuators are also operated at low voltage, so they can be easily integrated with simple off-the-shelf electronic components. Ultimately, the NiTi actuator driven 3D printed mechanisms have a great potential to be applied in a variety of microrobotic systems. In this work, the microgripper was fully released from the silicon wafer and glued to a printed circuit board (PCB) to demonstrate an integrated microgripper system. The adaptive gripper was used for the integration since it can provide more conformal gripping. The PCB was glued to a 3D-printed handle (Pico2 HD, Asiga), which was then connected to a circuit through enamel-coated copper wires. A current regulating circuit was designed using a voltage regulator (LM317MABTG, onsemi), and the circuit was powered by a 9 V battery (Fig. 8(b)). Since the regulator can maintain the voltage potential difference between the V_{out} and the adjust pin to 1.25 V, a 160 Ω resistor was added between two pins to supply around 8 mA of constant current to the microgripper. This is a much smaller current than used in the previous characterization steps and Fig. 5. The majority of heat is lost through the silicon wafer underneath the actuators, so the temperature of the NiTi actuators in the integrated system without the silicon was higher at a given current. Thus, the change in gripper opening of the integrated system at 8 mA was similar to that of the gripper on silicon wafer at 20 mA. A push button switch was used to turn on and off the gripper. The voltage required for the NiTi actuators was 2.3 V at 8 mA which is much lower compared to other microactuators such as electrostatic or piezoelectric actuators [22], [23], [28], [29]. The low voltage requirement

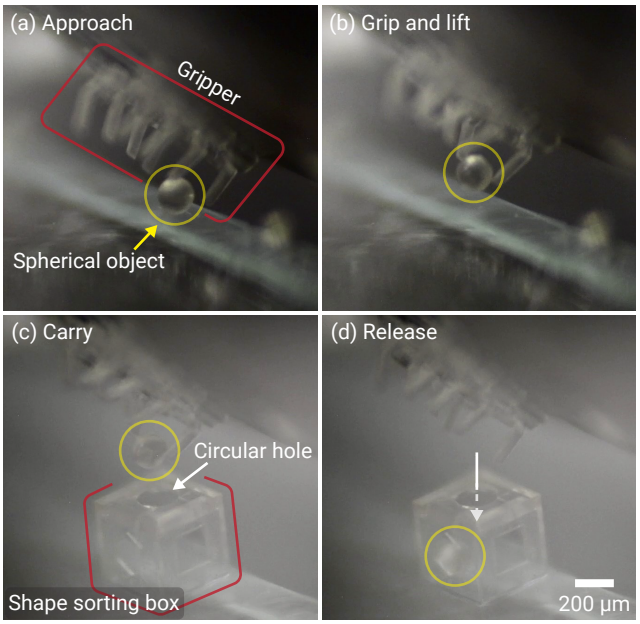

Fig. 9. Demonstration of a pick and place task using the integrated microgripper system. (a) The microgripper approached to a spherical object. (b) The microgripper gripped and lifted the object. (c) The microgripper carried the object to a microscale shape sorting box at a target location. (d) The microgripper released the object which went into the shape sorting box through a circular hole.

in actuation enabled the integration with the simple circuit and the off-the-shelf battery.

The integrated microgripper was able to grip objects with various shapes (Fig. 1). A book, a ball, and a bolt were 3D-printed with TPP for test objects, and each object represented a cuboid, a sphere, and a cylinder. Furthermore, a pick and place task was performed with the integrated microgripper and stills were captured from a video as shown in Fig. 9. A microscopic lens (Infinity Photo-Optical) was used with the DSLR camera to record the video. For the first time, the microgripper played with a microscale shape sorting box. A 190 µm microsphere and the shape sorting box were 3D-printed with TPP, and the task was to put the microsphere into a circular hole of the shape sorting box. The handle of the integrated system was fixed to a probe manipulator (XYZ 500, Quater Research) to precisely control the position of the microgripper. First, the microgripper approached to the spherical object (Fig. 9(a)). Then the push button switch was pressed down to actuate the microgripper and grip the object. The object was lifted from the ground while gripping (Fig. 9(b)). The microgripper then carried the object to the shape sorting box (Fig. 9(c)). Once the gripper was over the circular hole, the push button switch was released to turn off the microgripper. The spherical object was released from the microgripper and fell into the shape sorting box (Fig. 9(d)).

Releasing a microscale object is often difficult due to relatively large adhesive forces between the object and the gripper at the microscale. Therefore, microgrippers have often been integrated with ultrasonic fields, adhesive forces, and mechanical stops to successfully release objects [21], [30], [31]. The adaptive microgripper in this work was able to release the objects without any external intervention for most of the trials because of the 3D design of the fingers. The round finger design allowed for the contact area to be minimized resulting in smaller surface forces between the object and the gripper.

IV. CONCLUSION

This work presented a 3D-printed adaptive microgripper integrated with thin-film NiTi shape memory alloy actuators. To the best of our knowledge, it is the first time demonstrating a 3D-printed actuated linkage mechanism at the microscale. While a rigid gripper design with connected fingers resulted in a simple one DoF gripper, an adaptive gripper's finger mechanisms were able to move independently from each other and provide conformal gripping on an object. The adaptive gripper's opening changed by 225 µm when 20 mA was applied to the actuators on the silicon substrate, and each finger generated 30 µN of a blocking force.

In addition, the adaptive microgripper was released from a silicon wafer and was integrated with a PCB and a current regulating circuit. Since the NiTi actuator operates at low voltage, a commercial 9 V battery was used to power the whole system. The integrated microgripper demonstrated gripping microscale objects with various shapes. Furthermore, the microgripper was able to play with a shape sorting box at the microscale for the first time which requires a sufficient gripping and releasing capability.

One of the key contributions of this work is the use of thin-film NiTi along with 3D printing with TPP to create microscale actuated mechanisms with complex 3D geometries. This approach opens up a significant design space for microrobots. Future microrobots can take advantage of various linkage mechanisms that were only available at the macroscale. Another contribution is the adaptive gripper design. 8 fingers could passively adapt to an object's shape with a single actuation input. This principle can be beneficial for small scale robots since computation, actuation, and power resources are often limited at these scales. The final contribution is the fully integrated microgripper system. A combination of the fabrication method and NiTi microactuators enabled a simple integration with off-the-shelf electronics. By taking advantage of the method, various microrobotic systems including microgrippers or other mechanisms can be integrated with on-board batteries, sensors, and microcontrollers to achieve higher robot autonomy.

ACKNOWLEDGMENT

The authors would like to thank the staffs of Claire & John Bertucci Nanotechnology Laboratory and Soft Lithography lab at Carnegie Mellon University for their assistance in microfabrication and 3D printing. We would also like to thank Dr. Cory Knick and Dr. Gabriel Smith at the Army Research Lab for assistance in fabricating the NiTi films used in this work.

REFERENCES

[1] R. St.Pierre and S. Bergbreiter, "Toward autonomy in sub-gram terrestrial robots," *Annual Review of Control, Robotics, and Autonomous Systems*, vol. 2, pp. 231–252, 2019.

[2] D. S. Contreras and K. S. Pister, "A six-legged mems silicon robot using multichip assembly," in *Hilton Head Workshop*, 2018.

[3] P. Bhushan and C. Tomlin, "An insect-scale self-sufficient rolling microrobot," *IEEE Robotics and Automation Letters*, vol. 5, no. 1, pp. 167–172, 2019.

[4] K. Jayaram, J. Shum, S. Castellanos, E. F. Helbling, and R. J. Wood, "Scaling down an insect-size microrobot, hamr-vi into hamr-jr," in *2020 IEEE International Conference on Robotics and Automation (ICRA)*, pp. 10305–10311, IEEE, 2020.

[5] G.-P. Jung, J.-S. Koh, and K.-J. Cho, "Underactuated adaptive gripper using flexural buckling," *IEEE Transactions on Robotics*, vol. 29, no. 6, pp. 1396–1407, 2013.

[6] C. B. Schindler, J. T. Greenspun, H. C. Gomez, and K. S. Pister, "A jumping silicon microrobot with electrostatic inchworm motors and energy storing substrate springs," in *2019 20th International Conference on Solid-State Sensors, Actuators and Microsystems & Eurosensors XXXIII (TRANSDUCERS & EUROSENSORS XXXIII)*, pp. 88–91, IEEE, 2019.

[7] H. Ceylan, I. C. Yasa, O. Yasa, A. F. Tabak, J. Giltinan, and M. Sitti, "3d-printed biodegradable microswimmer for theranostic cargo delivery and release," *ACS nano*, vol. 13, no. 3, pp. 3353–3362, 2019.

[8] R. St.Pierre, W. Gosrich, and S. Bergbreiter, "A 3d-printed 1 mg legged microrobot running at 15 body lengths per second," in *Solid-State Sensors, Actuators, and Microsystems Workshop, Hilton Head, SC*, vol. 3, 2018.

[9] D. Kim, Z. Hao, J. Ueda, and A. Ansari, "A 5 mg micro-bristle-bot fabricated by two-photon lithography," *Journal of Micromechanics and Microengineering*, vol. 29, no. 10, p. 105006, 2019.

[10] S. Kim, C. Velez, R. St. Pierre, G. L. Smith, and S. Bergbreiter, "A two-step fabrication method for 3d printed microactuators: Characterization and actuated mechanisms," *Journal of Microelectromechanical Systems*, vol. 29, no. 4, pp. 544–552, 2020.

[11] S. Kim and S. Bergbreiter, "Fabrication and characterization of 3d printed out-of-plane torsional comb-drive actuators for microrobotics," in *2021 21st International Conference on Solid-State Sensors, Actuators and Microsystems (Transducers)*, pp. 6–9, IEEE, 2021.

[12] C. Velez, D. K. Patel, S. Kim, M. Babaei, C. R. Knick, G. L. Smith, and S. Bergbreiter, "Hierarchical integration of thin-film niti actuators using additive manufacturing for microrobotics," *Journal of Microelectromechanical Systems*, vol. 29, no. 5, pp. 867–873, 2020.

[13] C. Velez, S. Kim, M. Babaei, D. K. Patel, C. Knick, G. Smith, and S. Bergbreiter, "Rapid prototyping of microactuators by integrating 3d printed polymeric structures with niti thin film," in *2020 IEEE 33rd International Conference on Micro Electro Mechanical Systems (MEMS)*, pp. 893–896, IEEE, 2020.

[14] M. Power, A. J. Thompson, S. Anastasova, and G.-Z. Yang, "A monolithic force-sensitive 3d microgripper fabricated on the tip of an optical fiber using 2-photon polymerization," *Small*, vol. 14, no. 16, p. 1703964, 2018.

[15] P. S. Sreetharan, J. P. Whitney, M. D. Strauss, and R. J. Wood, "Monolithic fabrication of millimeter-scale machines," *Journal of Micromechanics and Microengineering*, vol. 22, no. 5, p. 055027, 2012.

[16] M. Karpelson, G.-Y. Wei, and R. J. Wood, "A review of actuation and power electronics options for flapping-wing robotic insects," in *2008 IEEE international conference on robotics and automation*, pp. 779–786, IEEE, 2008.

[17] K. Liu, C. Cheng, Z. Cheng, K. Wang, R. Ramesh, and J. Wu, "Giant-amplitude, high-work density microactuators with phase transition activated nanolayer bimorphs," *Nano letters*, vol. 12, no. 12, pp. 6302–6308, 2012.

[18] C. R. Knick, D. J. Sharar, A. A. Wilson, G. L. Smith, C. J. Morris, and H. A. Bruck, "High frequency, low power, electrically actuated shape memory alloy mems bimorph thermal actuators," *Journal of Micromechanics and Microengineering*, vol. 29, no. 7, p. 075005, 2019.

[19] M. Babaei, S. Kim, C. Velez, D. K. Patel, and S. Bergbreiter, "Increasing the energy efficiency of niti unimorph actuators with a 3d-printed passive layer," *Journal of Microelectromechanical Systems*, vol. 29, no. 5, pp. 797–803, 2020.

[20] J. Haringx, "The cross-spring pivot as a constructional element," *Flow, Turbulence and Combustion*, vol. 1, no. 1, pp. 313–332, 1949.

[21] M. Leveziel, W. Haouas, G. J. Laurent, M. Gauthier, and R. Dahmouche, "Migribot: A miniature parallel robot with integrated gripping for high-throughput micromanipulation," *Science Robotics*, vol. 7, no. 69, p. eabn4292, 2022.

[22] F. Beyeler, D. J. Bell, B. J. Nelson, Y. Sun, A. Neild, S. Oberti, and J. Dual, "Design of a micro-gripper and an ultrasonic manipulator for handling micron sized objects," in *2006 IEEE/RSJ International Conference on Intelligent Robots and Systems*, pp. 772–777, IEEE, 2006.

[23] A. Moreno, A. Patel, D. Teal, H. C. Gomez, A. Fearing, J. S. Rentmeister, J. Stauth, and K. Pister, "Small autonomous robot actuator (sara): A solar-powered wireless mems gripper," in *2021 IEEE International Conference on Robotics and Automation (ICRA)*, pp. 7227–7233, IEEE, 2021.

[24] S. Miyazaki and K. Otsuka, "Deformation and transition behavior associated with ther-phase in ti-ni alloys," *Metallurgical Transactions A*, vol. 17, no. 1, pp. 53–63, 1986.

[25] A. Kumar, D. Singh, and D. Kaur, "Grain size effect on structural, electrical and mechanical properties of niti thin films deposited by magnetron co-sputtering," *Surface and Coatings Technology*, vol. 203, no. 12, pp. 1596–1603, 2009.

[26] A. M. Dollar and R. D. Howe, "The highly adaptive sdm hand: Design and performance evaluation," *The international journal of robotics research*, vol. 29, no. 5, pp. 585–597, 2010.

[27] L. U. Odhner, L. P. Jentoft, M. R. Claffee, N. Corson, Y. Tenzer, R. R. Ma, M. Buehler, R. Kohout, R. D. Howe, and A. M. Dollar, "A compliant, underactuated hand for robust manipulation," *The International Journal of Robotics Research*, vol. 33, no. 5, pp. 736–752, 2014.

[28] M. Carrozza, A. Menciassi, G. Tiezzi, and P. Dario, "The development of a liga-microfabricated gripper for micromanipulation tasks," *Journal of Micromechanics and Microengineering*, vol. 8, no. 2, p. 141, 1998.

[29] P. B. Chu and S. Pister, "Analysis of closed-loop control of parallel-plate electrostatic microgrippers," in *Proceedings of the 1994 IEEE International Conference on Robotics and Automation*, pp. 820–825, IEEE, 1994.

[30] R. Pelrine and A. Hsu, "Magnetic pick, mechanical place on small scales," in *2022 International Conference on Manipulation, Automation and Robotics at Small Scales (MARSS)*, pp. 1–7, IEEE, 2022.

[31] F. Beyeler, A. Neild, S. Oberti, D. J. Bell, Y. Sun, J. Dual, and B. J. Nelson, "Monolithically fabricated microgripper with integrated force sensor for manipulating microobjects and biological cells aligned in an ultrasonic field," *Journal of microelectromechanical systems*, vol. 16, no. 1, pp. 7–15, 2007.